LIMNOLOGY and OCEANOGRAPHY

ASLO

Limnol. Oceanogr. 65, 2020, 979–991

doi: 10.1002/lno.11364

Glomalin-related soil protein distributions in the wetlands of the Liaohe Delta, Northeast China: Implications for carbon sequestration and mineral weathering of coastal wetlands

Lixin Pei,[1,2,3,4] Siyuan Ye ,[2,4,5*] Hongming Yuan,[2,4] Shaofeng Pei,[2,4] Shucheng Xie,[1] Jin Wang[2,4]

[1]School of Earth Sciences, China University of Geosciences (Wuhan), Wuhan, China
[2]Laboratory for Marine Geology, Qingdao National Laboratory for Marine Science and Technology, Qingdao, China
[3]Chinese Academy of Geological Sciences, Beijing, China
[4]Key Laboratory of Coastal Wetlands Biogeosciences, Qingdao Institute of Marine Geology, China Geologic Survey, Qingdao, China
[5]Shandong University of Science and Technology, Qingdao, China

Abstract

Arbuscular mycorrhizal fungi (AMF) is presumably to be associated with carbon sequestration and nutrient acquisition through mineral weathering in wetland ecosystems. However, information on AMF-carbon-weathering interactions is limited. Grain size, concentrations of nutrients, and the major components of 304 surface sediment samples and glomalin-related soil protein (GRSP) in 133 surface sediment samples were analyzed in various environments, including the upper delta plain wetlands (UDPW) and its adjacent shallow sea wetlands (SSW), to evaluate the relationship among the GRSP, carbon content, nutrients, and chemical index of alteration (CIA) in the wetlands of the Liaohe Delta (LHD). The concentrations of GRSP in surface sediments ranged between ~ 0.11 and 11.31 mg g^{-1}, with an average of 2.30 ± 0.17 mg g^{-1}, and were significantly affected by the vegetation types. The ratios of organic carbon in GRSP (GRSP-C) to soil organic carbon (SOC) varied from 0.71% to 25.34%, with an average of 10.34% ± 0.52%, indicating that the GRSP was an important carbon pool in sediments, and the carbon dynamics in these wetlands were closely related to human activities. Moreover, the CIA values ranged from ~ 18.97 to 68.75, and were significantly higher in the UDPW than in the SSW ($p < 0.05$), and were significantly correlated with the concentrations of GRSP (r^2 = 0.22 [r = 0.43], $p < 0.01$). Meanwhile, both the CIA and GRSP were significantly correlated with SOC, Total Nitrogen, and Fe ($r^2 > 0.17$ [$r > 0.41$], $p < 0.01$). The results indicate that AMF excursions in wetland ecosystems enhance carbon sequestration and mineral weathering, and in turn they alter retention of at least some nutrients.

One of the important ecosystem services provided by coastal wetlands is carbon and nutrient retention (Mitsch and Gosselink 2007). A key contribution to the formation and stabilization of carbon in soil aggregates, and presumably to the acquisition of mineral nutrients via enhanced weathering, is made by arbuscular mycorrhizal fungi (AMF) (Rillig 2004; Arocena et al. 2012), a plant-associated soil fungus, which may have a symbiotic association with 80% of vascular plant species (Wright et al. 1996).

The role of AMF in conditioning soils is achieved by its metabolite glomalin. That role is believed to include enhancement of soil aggregate stability (Xie et al. 2015), maintenance of soil fertility (Singh et al. 2016), and enhancement of soil carbon capture (Rillig 2004; Wang et al. 2018*b*). Therefore, a proxy for AMF, glomalin-related soil protein (GRSP), has been widely used to explore the role of AMFs in various ecosystems around the world (Lovelock et al. 2004; He et al. 2010; Spohn and Giani 2010). However, glomalin has not been biochemically defined, it has often been quantified in terms of GRSP (Rillig 2004), which is a mixture of proteinaceous, humic, lipid, and inorganic substances that are derived via AMF senescence and microbial decomposition (Wright and Upadhyaya 1998; Driver et al. 2005). An important attribute of GRSP is that has longer turnover time (~ 40–100 yr) and lower degradation rate than other organic matter under natural conditions, especially under reducing conditions (Rillig et al. 2003*b*; López-Merino et al. 2015). Therefore, GRSP could function as a metric of AMF excursions in the sediments of coastal wetlands.

Microscopic observations of the roots of wetland plants and genomic analyses with specific DNA primers have

*Correspondence: siyuanye@hotmail.com

Additional Supporting Information may be found in the online version of this article.

evidenced that AMF are widespread on the roots of many wetland plants across a variety of wetlands (Caravaca et al. 2005; Xu et al. 2016), and GRSP can be transported in water through their association with soil particles (Harner et al. 2004; Adame et al. 2010; Singh et al. 2017). Based on this information and the redox characteristics of wetlands (Ye et al. 2015), GRSP should be widely distributed in wetland sediments, and the size of the GRSP pool might be very large.

GRSP is an important adhesive for the formation of soil aggregates (Wright and Upadhyaya 1998). Some studies have revealed that the concentration of GRSP is positively correlated with the abundance of soil water-stable aggregates (Spohn and Giani 2010), and the aggregates of soil particles can enhance the efficiency of carbon storage (Rillig 2004). GRSP may therefore play an important role in long-term carbon sequestration in coastal wetlands. However, there have been few quantitative assessments of the distribution of GRSP and of its role in carbon sequestration in coastal wetlands, especially deltaic wetlands.

Mineral weathering is a fundamental geochemical process on the surface of the earth. A few studies have shown that mycorrhizal fungi play an important role in the weathering of rock minerals and the biogeochemical cycle of nutrients worldwide (Jongmans et al. 1997; Sanz-Montero and Rodríguez-Aranda 2012). Unlike ectomycorrhizal fungi (EMF), AMF are generally thought to not directly participate in mineral weathering, and only a few studies have explored their direct effect on the rate of mineral weathering under laboratory conditions (Johansen et al. 1993; Arocena et al. 2012). Some scientists have speculated theoretically that respiration by AMF could affect mineral weathering by releasing hydrogen ions and nutrients, and this release could in turn affect the pH and nutrient content of soil pore water and facilitate direct absorption of NH_4-N by plants (Bago et al. 1996). AMF secretions may also increase the weathering of minerals by increasing the number of soil aggregates (Wilson et al. 2009) or by stimulating biological and chemical processes associated with soil particles. Moreover, AMF may form a thin film that covers the surface of mineral particles and thereby reduce the chance of their exposure to weathering and hinder interactions between water and minerals (Kleber et al. 2007). However, there is no evidence from field observations to support the aforementioned hypotheses.

In this study, we characterized the spatial distributions of GRSP in surface sediments across various land uses within the 3606 km^2 of deltaic wetlands in the Liaohe Delta (LHD), Northeastern China. We tested the following two hypotheses: (1) GRSP is widely present in the surface sediments of coastal wetlands and promotes carbon sequestration and (2) AMF in wetland ecosystems influences mineral weathering and alters nutrient retention. We then explored factors affecting the distribution of GRSP in wetlands with the expectation that effective measures might be identified to enhance their role in nutrient retention and carbon storage.

Materials and methods

Site description and sampling

The Liaohe Delta (121°7′E–122°24′E, 40°20′N–41°19′N) is located in the southwest of the Liaoning province, northeast China, and has been formed by sediments deposited from the Liaohe, Daling, Xiaoling, Daliao, and Daqing Rivers. The delta is located in the northern temperate continental monsoon climate zone. The annual average temperature is 8.3–8.4°C. The annual average precipitation is 612–640 mm, > 60% of which occurs in the summer.

This study focused mainly on the upper delta plain wetlands (UDPW) and the shallow sea wetlands (SSW) of the delta. The UDPW of the Liaohe Delta has a total area of 3601 km^2. It includes the world's largest reed field (789 km^2), extensive rice paddies (2465 km^2), an intertidal and seablite wetland (33 km^2), and dry land (314 km^2). Most of the dry lands here were wetlands in the past, but they were later reclaimed as cornfields (Brix et al. 2014; Ye et al. 2016*a*). The average tidal range is 2.7 m according to the tide gauge station at the nearby Yinkou observatory (Ye et al. 2016*b*).

The dominant plant species in the Liaohe Delta wetlands are reed (*Phragmites australis*), rice (*Oryza sativa*), corn (*Zea mays Linn)*, and seablite (*Suaeda salsa)*. A total of 204 surface sediment (0–5 cm) samples were collected in the study area from July to August of 2012. Seventy-nine samples were collected from the rice paddy wetland, 52 from the reed wetland, 37 from the seablite wetland, and 36 from the corn field (Fig. 1). Prior to sampling, soil surface litters and stones were gently removed to expose bulk soil. The SSW of the Liaohe Delta refers to the area covered by seawater to a depth < 6 m at low tide. This area is in the northern part of the Liaodong Bay in the Bohai Sea. A total of 100 surface sediment (0–5 cm) samples from the SSW were collected using a stainless-steel grab (0.02 m^2) from June to July of 2013. All the collected samples were wrapped in foil and stored in an icebox during transport back to the laboratory of the Qingdao Institute of Marine Geology for analyses.

Physicochemical properties of the sediments

The soil pH was measured in a 1:5 sediment-to-water suspension over 24 h. The moisture content was determined from the loss of weight after drying ~ 35 g of soil. Grain size analyses were done with a Mastersizer 2000 Instrument (Malvern, UK) after removing carbonates with 5 mL of HCl solution (3 mol L^{-1}). The soil carbon and total nitrogen (TN) were analyzed with a CHNS analyzer (Vario EL III, Germany Elemental Cooperation) after being ground to 200 mesh. Total phosphorus (TP) was quantified by double acid digestion (HNO_3 + $HClO_4$) followed by colorimetric analysis (Olsen and Sommers 1982). Major components SiO_2, Al_2O_3, Fe_2O_3, CaO, MgO, Na_2O, K_2O, and Cl in surface sediments were determined with a PANalytical Axios PW4400 X-ray fluorescence spectrometer (Panaco Company, The Netherlands). The results were calibrated with GBW07315, a marine sediment standard sample. The certified values were generally < 5% in magnitude.

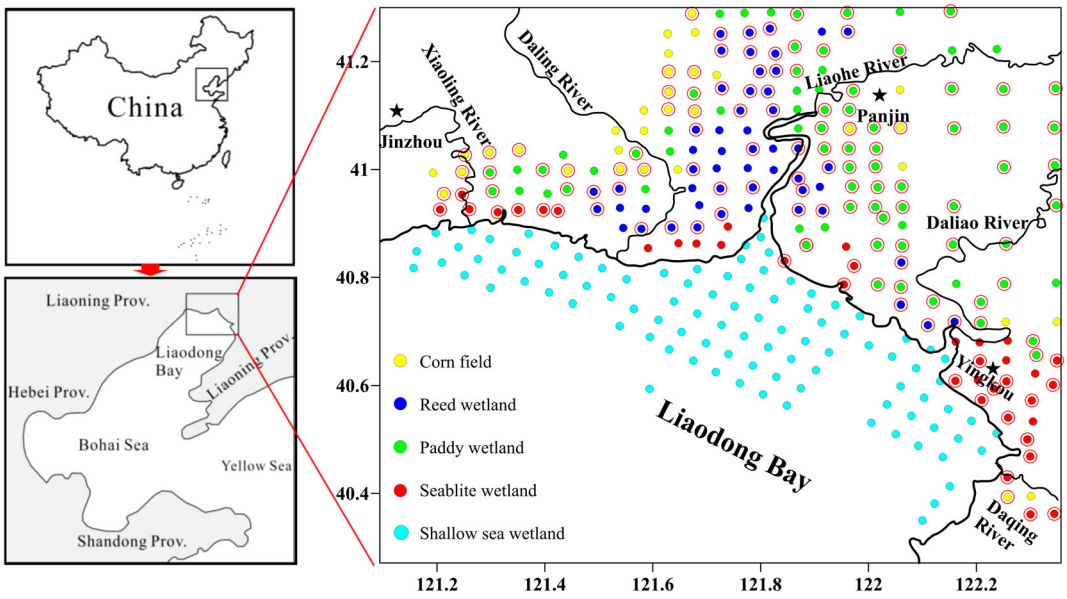

Fig. 1. Location of study area and sampling stations (the stations selected for GRSP analysis are circled in red).

GRSP

One hundred thirty-three surface sediment samples from the UDPW were selected for analysis of GRSP. A total of 56, 32, 25, and 20 samples were collected for chemical analysis from paddy fields, reed wetlands, seablite wetlands, and corn fields, respectively (Fig. 1). The analyses of the soil samples for GRSP were conducted as described by Wright et al. (2006). Briefly, 1–2 g of freeze-dried soil was extracted with 8 mL of 100 mmol L^{-1} sodium pyrophosphate at 121°C for 60 min. This procedure was repeated several times on the same sample until the extract was straw-colored. The supernatants from all replicates were pooled together and centrifuged at 10,000 × *g* for 10 min to remove soil particles. The GRSP extracts were then precipitated with 0.1 mol L^{-1} hydrochloric acid at a pH of 2.1, incubated in ice for 60 min, and centrifuged at 4000 rpm for 20 min. The precipitate was then redissolved in 0.1 mol L^{-1} sodium hydroxide to ensure complete reconstitution. The redissolved samples were transferred to dialysis bags (8–14 kDa) and placed in deionized water for dialyzing at 12-h intervals five times. The purified dialysate was centrifuged at 4000 rpm for 20 min to remove any extraneous particles. Part of the collected supernatant was used for determination of the GRSP concentration; the rest was immediately freeze-dried and subsequently analyzed for carbon content with a CHNS analyzer (Vario EL III, Germany Elementar Cooperation). The protein concentration was determined by the Bradford assay (Wright and Upadhyaya 1998) with a DS-1 FX spectrophotometer (DeNovix company, U.S.A.) using bovine serum albumin as a standard.

The chemical index of alteration and ternary diagrams

The chemical index of alteration (CIA) was first proposed by Nesbitt and Young (1982) and has been widely used as a proxy for reconstructing chemical weathering. The CIA is expressed as $CIA = [Al_2O_3/(Al_2O_3 + Na_2O + K_2O + CaO^*)] \times 100$, where CaO* is the calcium incorporated into silicate minerals. In this article, we adopted the calculation method recommended by McLennan (1993): $n(CaO') = n(CaO) - 10 \times n(P_2O_5)/3$; If $n(CaO') < n(Na_2O)$, then $n(CaO^*) = n(CaO')$, otherwise $n(CaO^*) = n(Na_2O)$, where "n" stands for molecular content.

The effects of weathering and sorting sediments were determined by comparing the bulk compositions and mineralogy of the sediments. However, direct comparisons and mass balances cannot be achieved by using single variables. Instead, we used ternary diagrams, on which the bulk compositions could be plotted and related to mineralogy for all sediments. An A-CN-K diagram depicts the molar proportion of Al_2O_3 (A apex), $CaO^* + Na_2O$ (CN apex), and K_2O (K apex). An A-CNK-FM diagram reveals the molar proportions of Al_2O_3 (A apex), $CaO^* + Na_2O + K_2O$ (CNK apex), and $FeO_T + MgO$ (FM apex) (Nesbitt et al. 1996).

Data analyses were performed with MATLAB® and R software (http://www.r-project.org).

Results

Grain size

Figure 2a,b shows the grain size distributions of sediments in the UDPW and SSW. The surface sediments of the UDPW could be clustered into four types: silt, sandy mud, sandy silt, and silty sand. The silt and sandy mud were distributed along the Liaohe River and the Daliao River floodplains, which were dominated by reed and paddy wetlands. The sandy silt and silty sand were distributed along the Daling and Xiaoling River floodplains, which were close to the source of the material. However, in the case of

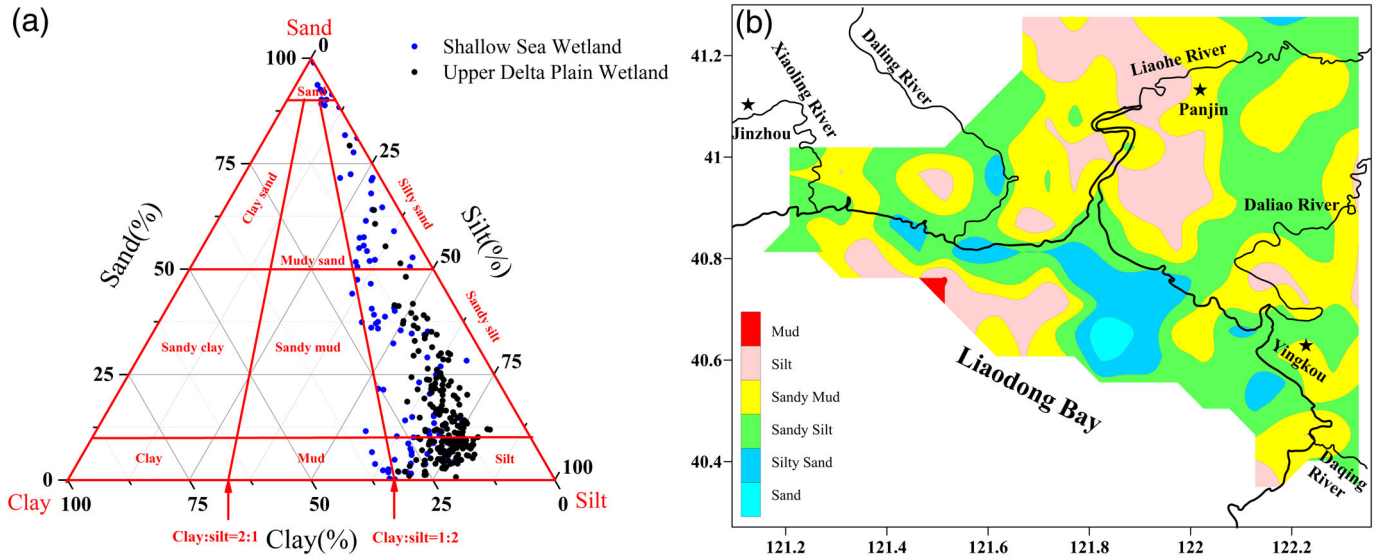

Fig. 2. Ternary map of grain size classification (**a**) and the spatial variations of sedimentary categories (**b**). Figure modified from Liu et al. (2017).

the SSW wetland, there were six types of sediments—mud, silt, sandy mud, sandy silt, silty sand, and sand—which were less sorted than the UDPW sediments. The spatial distribution of sediment categories in the SSW could be divided into three fractions: western fine-grained silt and sandy mud, central coarse-grained silty sand and sand, and eastern middle-sized sandy silt.

Chemical characteristics

The CIA values and nutrient (SOC, TN, TP, and Fe) concentrations averaged over all the 204 samples were consistently higher in the UDPW (Table 1), but in most cases the ratios of the average values in the UDPW to the average values in the SSW were less than 2.3. The average concentrations of major components SiO_2, Al_2O_3, CaO, and MgO were comparable in these two very different landscapes. However, there were two exceptions. In the SSW sediments, concentrations of Na and Cl were 2.3 and 3.9 times the analogous concentrations in UDPW (Table 1). Remarkably, the average concentrations of $SiO_2 + Al_2O_3$ exceeded 74% in both the UDPW and SSW, whereas the average concentrations of other elements were less than 5% (Table 1).

Table 1. Major components and grain size characteristics of sediments in the Liaohe Delta.

	Upper delta plain wetland					Shallow sea wetland				
Chemical parameters	**Mean**	**Max**	**Min**	**SD**	**CV (%)**	**Mean**	**Max**	**Min**	**SD**	**CV (%)**
TN (mg g^{-1})	0.97	3.80	0.16	0.44	45.54	0.49	1.03	0.10	0.20	41.66
TP (mg g^{-1})	0.66	1.93	0.32	0.19	28.84	0.47	0.76	0.25	0.09	20.03
Fe (mg g^{-1})	32.39	54.74	13.51	7.60	23.48	28.23	49.07	10.43	9.68	34.30
TC (mg g^{-1})	13.29	56.70	2.60	7.90	59.43	6.84	13.60	2.30	2.74	40.05
SOC (mg g^{-1})	10.64	49.00	1.70	6.47	60.74	4.51	9.70	1.10	1.99	44.26
GRSP (mg g^{-1})	2.30	11.31	0.11	1.92	83.48	ND	ND	ND	ND	ND
GRSP-C/SOC (%)	10.34	25.34	0.72	6.00	58.03	ND	ND	ND	ND	ND
Cl (mg g^{-1})	1.10	15.66	0.06	2.47	223.18	4.29	12.09	0.63	2.15	50.22
SiO_2 (%)	63.40	75.30	36.56	3.89	6.13	62.24	80.62	36.11	8.52	13.70
Al_2O_3 (%)	13.54	17.59	9.07	1.28	9.44	12.13	15.08	8.20	1.37	11.29
MgO (%)	1.90	5.22	0.61	0.48	25.22	1.64	2.62	0.54	0.52	31.91
CaO (%)	1.93	17.30	0.76	1.30	67.25	1.99	16.51	0.80	1.52	76.50
Na_2O (%)	2.12	5.75	1.22	0.72	33.92	4.92	21.18	2.16	4.07	82.76
K_2O (%)	2.86	3.78	1.40	0.20	6.97	3.07	3.64	2.14	0.20	6.60
CIA	58.87	68.75	36.61	5.37	9.12	46.54	57.64	18.97	8.95	19.23

CV, coeficient of variation; GRSP-C, carbon concentration of the GRSP; ND, not determined; SD, standard deviation; SOC, sediment (soil) organic carbon; TN, total nitrogen; TP, total phosphorus;.

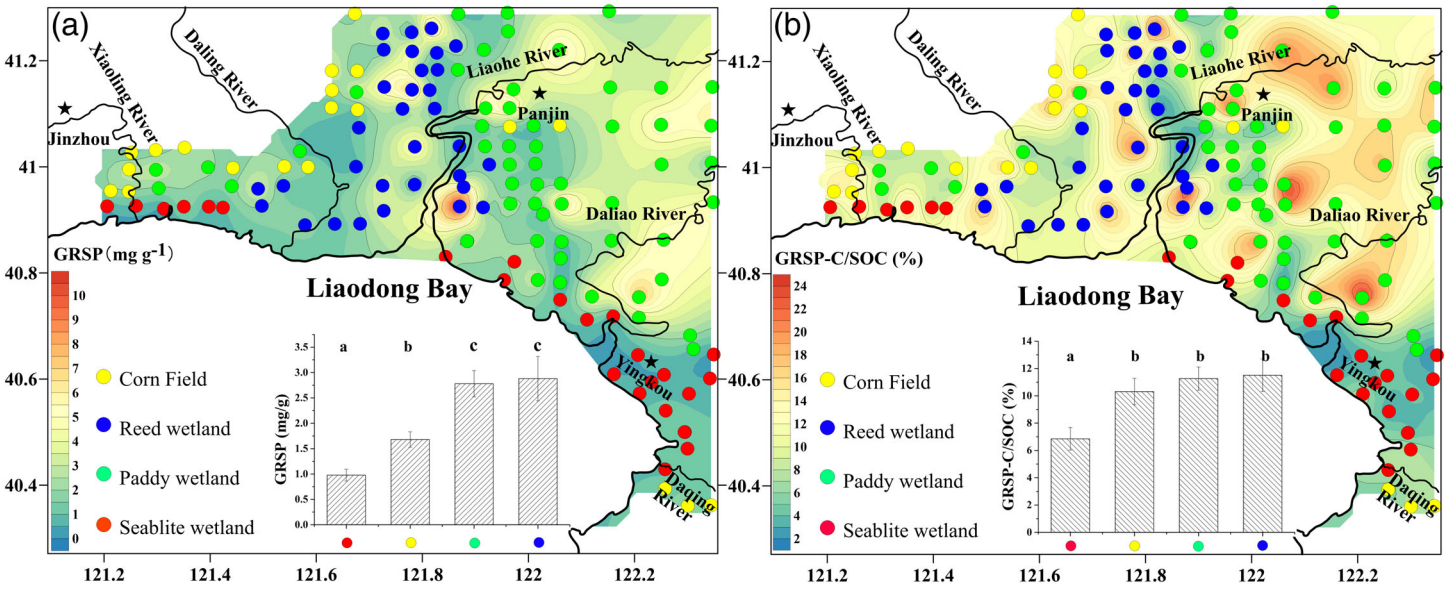

Fig. 3. Spatial variations of GRSP (**a**) and GRSP-C/SOC (**b**) in the sediments of the Liaohe Delta.

The distributions of GRSP, soil organic carbon, and the GRSP/soil organic carbon ratio

The GRSP concentrations averaged over 133 samples were 2.30 ± 0.17 mg g^{-1}. The concentrations associated with the different kinds of land use were (in descending order) reed wetland (2.88 ± 0.44 mg g^{-1}) ≈ paddy wetland (2.78 ± 0.26 mg g^{-1}) > corn field (1.68 ± 0.15 mg g^{-1}) > seablite wetland (0.98 ± 0.12 mg g^{-1}) (Table 1, Fig. 3a, where ≈ indicates no significant difference). The highest GRSP concentrations were generally found in the floodplains of the Liaohe and Daliao rivers, where the dominant landscapes were reed and paddy wetlands, followed by corn fields; the lowest concentrations were along the shoreline in the seablite wetlands (Fig. 3a). In addition, GRSP concentrations were always lower in the SSW than in seablite wetlands (Adame et al. 2010; Wang et al. 2018*a*).

In this study, 20 extracted GRSP samples were selected randomly for C concentration analysis. The average C concentration of the GRSP (GRSP-C) was 42% ± 1% (range 34–49%) (Supporting Information Table S1), which was within the current literature range of 19–52% (Gillespie et al. 2011; Wang et al. 2014). The soil organic carbon (SOC) concentrations varied from 1.7 to 29.9 mg g^{-1} (Supporting Information Table S2) and averaged 9.4 ± 0.41 mg g^{-1}. The GRSP-C/SOC percentages varied from 0.71% to 25%, with an average of 10.4% ± 0.52%. The average GRSP-C/SOC ratios among the vegetation types varied in the order reed wetland (11.5% ± 1.2%) ≈ paddy wetland

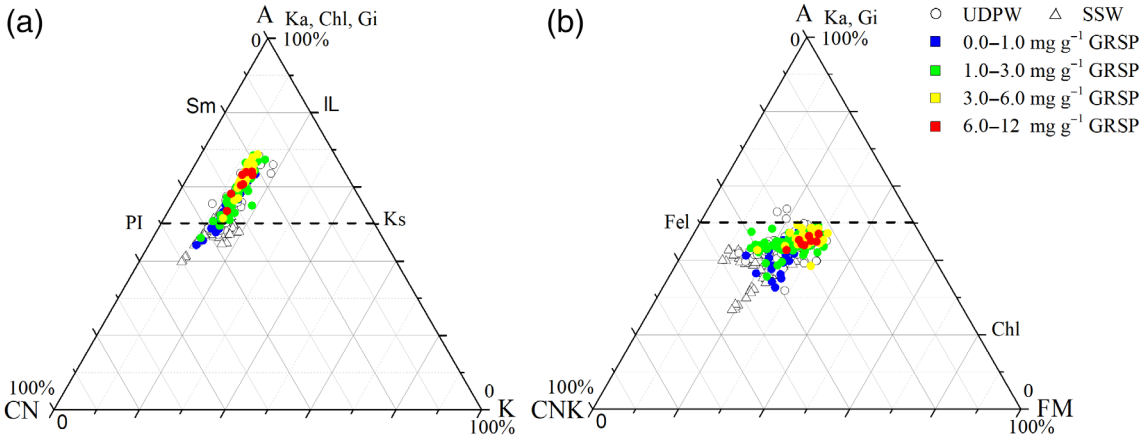

Fig. 4. The A-CN-K (**a**) and A-CNK-FM (**b**) chemical weathering trend chart (Ka = kaolinite; Chl = chlorite; Gi = gibbsite; Sm = smectite; IL = Illite; Pl = plagioclase; Ks = K-feldspar; Fel = feldspar; A = Al_2O_3; CN = CaO* + Na_2O; K = K_2O; CNK = CaO* + Na_2O + K_2O; FM = FeO(T) + MgO).

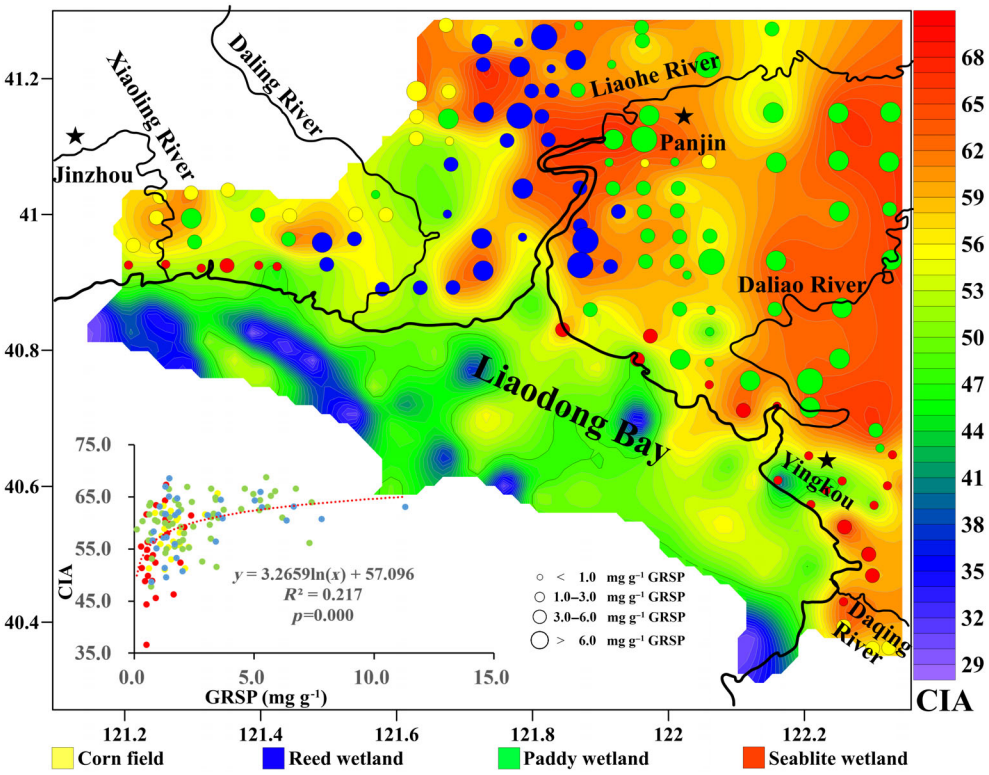

Fig. 5. Spatial variations of CIA in the sediments of the Liaohe Delta.

(11.3% ± 0.85%) ≈ cornfield (10.3% ± 0.97%) > seablite wetland (6.9% ± 0.83%) (Fig. 3b). A remarkable finding was that the seablite wetland contained a significantly lower GRSP-C/SOC ratio than the other habitats ($p < 0.01$, Fig. 3b).

Chemical weathering

The trend chart of A-CN-K chemical weathering (Fig. 4a) showed that the weathering trend of the sediments followed a line parallel to the A-CN boundary and close to plagioclase (Pl). The highest GRSP concentrations (> 3 mg g^{-1}) were close to the A apex. Meanwhile, the pattern of chemical weathering on the A-CNK-FM diagram (Fig. 4b) revealed that the CNK values were highly differentiated. The bulk sediment compositions with high GRSP concentrations were close to the composition of feldspar (Fel) join.

CIA and its relationships with GRSP, nutrients, and stressors

The CIA was used to classify weathering levels as follows: unweathered (CIA < 50), primary weathering (CIA = 50–64),

Table 2. Pearson correlation coefficients (r) and goodness of fit (r^2) between GRSP (CIA) and sediment physicochemical properties in the LHD (n = 133 samples for GRSP correlations; n = 204 samples for CIA correlations).

Variables	GRSP	CIA	SOC	WC	BD	Sand	Silt	Clay	pH
GRSP	1**	0.43**	0.56**	0.55**	−0.57**	−0.26**	0.22*	0.25**	−0.12
	(1)	(0.22)	(0.31)	(0.30)	(0.32)	(0.07)	(0.05)	(0.06)	(0.02)
CIA	0.43**	1**	0.59**	0.45**	−0.58**	−0.45**	0.41**	0.37**	−0.20*
	(0.22)	(1)	(0.35)	(0.20)	(0.33)	(0.20)	(0.17)	(0.14)	(0.04)
Variables	**Na**	**K**	**Ca**	**Mg**	**TN**	**TP**	**S**	**Cl**	**Fe**
GRSP	−0.36**	−0.16	−0.02	0.17**	0.45**	0.32**	−0.07	−0.21*	0.41**
	(0.13)	(0.02)	(0.00)	(0.03)	(0.21)	(0.10)	(0.00)	(0.04)	(0.17)
CIA	−0.87**	−0.14	−0.12	0.39**	0.62**	0.28**	−0.38**	−0.59**	0.74**
	(0.76)	(0.02)	(0.01)	(0.15)	(0.38)	(0.08)	(0.15)	(0.35)	(0.55)

SOC, sediment (soil) organic carbon; TN, total nitrogen; TP, total phosphorus; WC, water content.
*$p < 0.05$; **$p < 0.01$.

moderate weathering (CIA = 65–85), and intense weathering (CIA > 85) based on the weathering classification proposed by Nesbitt and Young (1982). The CIA value averaged over 204 samples in the UDPW was 59, with a range of 37–69. About 84% of the surface sediments in the UPDW were assigned to the primary weathering category; 10%—in the floodplain of the Liaohe River and Daliao River—were classified as moderately weathered; and 6%—right on the coastlines or near the mountain area—were classified as unweathered. In the SSW, the CIA ranged from 19 to 58 and averaged 47, and 56% and 44% of the samples were assigned to the unweathered and primary weathering categories, respectively. No samples were assigned to the moderate or intense weathering categories (Fig. 5). The CIA was significantly correlated with GRSP concentrations ($r^2 = 0.22$, $p < 0.01$) (Fig. 5). Both the CIA and GRSP were significantly correlated with nutrient concentrations (SOC, TN, TP, and Fe), sediment structure (moisture, bulk density [BD], and grain size), and environmental stressors (Na, Cl) ($p < 0.01$) (Table 2).

Discussion

GRSP distributions and its implication for carbon sequestration

GRSP concentrations among different ecosystems and land uses might be affected by a variety of factors, including climate, soil properties, vegetation types, primary productivity, and AMF species and their abundance (Rillig 2004; Treseder and Turner 2007). The results of our study provided important evidence that supported our hypothesis that GRSP is widely present in the surface sediments of coastal wetlands (Fig. 3a) and that it promotes carbon sequestration (Fig. 3b). These values (0.11–11.31 mg g^{-1}) were comparable to those in mangrove forests, agricultural lands, and tropical forests (1.5–13.5 mg g^{-1}) (Wright and Anderson 2000; Lovelock et al. 2004; Singh et al. 2013; Wang et al. 2018*b*). However, the values were significantly higher than the GRSP concentrations in deserts (0.68–1.18 mg g^{-1}) (Bai et al. 2009) and semiarid grasslands (0.25–1.8 mg g^{-1}) (Bird et al. 2002; Rillig et al. 2003*a*). The extensive distribution of GRSP in this area revealed that AMF colonization was widespread and was playing an active role in the preservation of organic carbon in sediments of the reed wetlands, paddy wetlands, and corn fields in this area. Supporting Information Fig. S1a shows that high SOC concentrations are usually associated with peaks of the GRSP distributions, and the correlation between SOC and GRSP concentrations was highly relevant and significant ($r^2 = 0.31$, $p = 2.36 \times 10^{-12}$). The implication is that GRSP is conducive to SOC preservation. However, the GRSP concentrations were not high in all of the deltaic wetlands; the concentrations in the seablite wetlands were remarkably low, presumably because of tidal effects (Fig. 3a).

The ratio of GRSP-C to SOC varied among ecosystems and typically reflected the extent of AMF colonization of vascular plants roots, organic carbon inputs, and environmental factors. GRSP is a relatively stable glycoprotein and biodegrades more slowly than other compounds that form SOC (Spohn and Giani 2010). The GRSP-C/SOC ratio therefore increases when soil is disturbed, for example, by farming activities. This phenomenon has been evidenced in several previous studies (Preger et al. 2007; Spohn and Giani 2010) and was the case in our study (Fig. 3b). The corn field and paddy wetland were disturbed by the annual cycle of soil preparation, planting, and harvesting, and the GRSP-C/SOC ratios in those soils could reach up to 12–25% (Fig. 3b), which are higher than the reported ratios of 3–12% in tropical rain forests, mudflats, mangroves, and semiarid grasslands (Bird et al. 2002; Lovelock et al. 2004; Wang et al. 2018*b*). The GRSP-C/SOC ratios should presumably have been no higher in the reed wetland than in the seablite wetland. However, that was not the case. In fact, the GRSP-C/SOC ratios in the reed wetlands were comparable to the ratios in the corn fields (Fig. 3b), and there was no significant difference between ratios in the reed wetlands and corn fields or paddy lands ($p > 0.20$). This similarity was probably related to the management of the reed wetlands. The reeds are harvested and used for paper making every year (Brix et al. 2014) in the study area. This human activity greatly reduces the input of organic matter into the sediment. The GRSP-C/SOC ratios were therefore high and not significantly different from the ratios in the paddy wetlands ($p > 0.54$) and corn fields ($p > 0.86$) (Fig. 3b).

Consideration of the fact that most of our sampling points were located in a floodplain of one or another of the five rivers that have formed the Liaohe Delta may also help to explain the high GRSP-C/SOC ratios. The most easily decomposed carbon transported by rivers is easily lost during long-distance transport. The remaining refractory carbon is enriched in GRSP-C, which is difficult to decompose. When this carbon settles out in the floodplain, the soil is enriched in allochthonous GRSP-C. We conclude that the dual mechanism of adding allochthonous GRSP-C during floods and reducing labile SOC via disturbances to the soil leads to a remarkable increase in the GRSP-C/SOC ratio in the sediments of the LHD (Fig. 3b).

The remarkably high GRSP-C/SOC ratios confirmed that GRSP was an important part of the sediment carbon pool in the LHD. However, the implications for carbon sequestration are not good. In fact, GRSP is a stable compound, insoluble in water and resistant to heat degradation (Wright et al. 1996). Because of its adhesive properties, it contributes to the formation of soil aggregates and helps to protect other forms of carbon in the soil (Wright and Upadhyaya 1998; Zhang et al. 2012). The implication is that higher GRSP concentrations protect carbon from degradation and thereby increase carbon sequestration in sediments. However, despite the high GRSP-C/SOC ratios in the sediments of the wetlands and croplands that we studied, the GRSP concentrations were not significantly higher (Supporting Information Tables S1, S2) than the analogous concentrations in many other ecosystems (Wright and Anderson 2000; Spohn and Giani 2010). Low GRSP concentrations are not conductive to soil aggregate formation and

carbon sequestration, and the high GRSP-C/SOC ratios suggest that a large amount of carbon may have been returned to the atmosphere or otherwise lost from these ecosystems. It is imperative that measures should be identified to improve AMF colonization and increase GRSP concentrations in these deltaic wetlands and farmlands.

Effects of AMF on sediment weathering characteristics

In order to explore the effect of AMF on weathering process, triangle maps were constructed to analyze the weathering characteristics of sediment samples with different GRSP concentrations. The A-CN-K and A-CNK-FM diagrams are currently used to represent the composition of clay mineral assemblages formed in different weathering stages. Based on the evolution of sediment chemical composition, Nesbitt et al. (1980) have divided the chemical weathering process into three stages: the Na, Ca-depletion stage (early stage), the K-depletion stage (intermediate stage), and the Si-depletion stage (late stage). According to Fig. 4a, the trend line of sediment weathering was basically parallel to the A-CN transition line and close to plagioclase. This pattern indicated that chemical weathering in the study area was either at a late Na, Ca-depletion stage or an early K-depletion stage, with a tendency toward plagioclase formation, whereas potassium feldspar remained almost constant across the SSW to UDPW transition. Because Ca and Na are essential elements for plant growth, the reduction of these two elements in sediments across the SSW–to–UDPW transition was likely due to the selective uptake of nutrients by plants in the sediments. Consistent with this scenario is the fact that Ca and Na in the soil of the vegetated reed wetland were significantly depleted. The implication is that plants play an important role in weathering. It is apparent from Fig. 4a that all the samples with GRSPs higher than ~ 3 mg g^{-1} was above PI-Ks line, and tended to approach the Sm-IL line because of the gradual depletion of Ca and Na. In addition, there was an apparent differentiation between mafic and felsic minerals in the study area, with the exception of a few samples from the SSW (Fig. 4b). This differentiation suggests preferential removal of the mafic components (Fe, Mg) and felsic minerals (Ca, Na) because wetland plants consume both felsic and mafic minerals during their growth (Fig. 4b). This assessment is consistent with Fig. 4a that all the samples with relatively high GRSP concentrations (> 3 mg g^{-1}) contained relatively low amounts of felsic minerals and tended to approach the Fel line (Fig. 4b).

The above diagrams indicated that biologically AMF-mediated weathering in this area leads to the formation of clay minerals, but no mineral assemblages of kaolinite, chlorite, or gibbsite has been formed. In other words, the sediments in the study area continuously provide the mineral nutrients needed for plant growth, and biological activity in turn stimulates the weathering of sediment minerals.

Many studies have shown that CIA values can reflect the chemical weathering intensity during sediment formation (Nesbitt et al. 1996). The low weathering intensities of the floodplains of the Daling River and Xiaoling River near the granite mountain (Fig. 5) (Yang et al. 2019) were probably due to the short length of the rivers and the low abundance of plants. However, in other vegetated areas of the UDPW, such as the reed wetlands, paddy wetlands, and corn fields, the intensities of chemical weathering were relatively high; in some areas, the CIA index (> 65) indicated that the degree of chemical weathering was moderate. Remarkably, there is an overall positive correlation between GRSP and CIA (r^2 = 0.22, $p < 0.01$), and this pattern may be explained by at least three possible mechanisms: (1) because GRSP is a colloidal glycoprotein produced by AMF, the glomalin concentration in sediment was positively correlated with the primary productivity of surface vegetation (Treseder and Turner 2007). High concentrations of GRSP indicate that the vegetation is growing vigorously, and under these conditions the root development of the plants has a stronger physical crushing effect on detrital materials (Berner 1997). Moreover, the uptake of elements such as Ca, Na, Fe, and Mg from sediments during plant growth (Fig. 4a,b) will enhance chemical weathering and lead to an increase of CIA values, (2) the high concentrations of GRSP indicate that the AMF are growing vigorously. AMF can presumably function as EMF and secrete organic acids that are directly involved in mineral weathering (Jongmans et al. 1997; Koele et al. 2014). Evidence in support of this hypothesis is the significant correlation between the CIA and pH ($p < 0.05$, Table 2), and (3) GRSP may accelerate mineral weathering by increasing the amount of soil aggregates or by enhancing the biological and chemical weathering that occurs between soil particles.

Although there is an overall positive correlation between GRSP and CIA, there is a large amount of scatter at low GRSP concentrations because weathering is controlled by other factors, such as physical transport, climate, and local environmental conditions (Mo and Lian 2010). However, at high GRSP concentrations, the relationship between weathering and GRSP is more deterministic, and there is much less scatter in the data. Weathering is controlled mainly by biological processes related to AMF activity. The CIAs are therefore high and positively correlated with GRSP concentrations. A simple probabilistic model (Supporting Information Fig. S4) can easily explain the pattern in Fig. 5.

Chemical weathering is an important mechanism for the acquisition of nutrients in an ecosystem and is an important process in the global biogeochemical cycle of nutrient elements (April and Newton 1992). In nature, essential plant nutrients such as P, K, Mg, and Fe need to be released from rocks and minerals by weathering and then absorbed by plants (Johnson et al. 1982). Our results showed that there were significant positive correlations between CIA and TN, TP, Mg, and Fe in the study area (Table 2, Supporting Information Figs. S1c,d, S3c,d), and the

p values were usually less than 0.01. These results are consistent with the assumption that chemical weathering facilitates the release of some nutrients from minerals (April and Newton 1992). It is particularly noteworthy that the Fe in the sediments explained ~ 55% of the CIA variance (Table 2). The fact that the r^2 between CIA and P in Table 2 is only 0.078 suggests that variations of P explain only ~ 8% of the CIA variance (Table 2). This low percentage implies that there are more sources of P than weathering or that demand for P (i.e., uptake of P by plants) obscured variations of P supply.

Environmental factors affecting accumulation of GRSP

Because GRSP is a protein produced by AMF, it contributes to the organic matter found in sediments (Wright et al. 1996). The concentrations of GRSP in soil depend on the combined effects of GRSP production and degradation. In this study, the relatively high concentrations of GRSP found in the paddy wetlands and reed wetlands (Fig. 3a) may be explained by one or more of the following three arguments: (1) the sediments in paddy wetlands and reed wetlands are submerged for a long time, and the anaerobic or dysoxic conditions contribute to the preservation and accumulation of GRSP (López-Merino et al. 2015), (2) rice and reeds are typical hydrophytes that could transport sufficient oxygen to their roots via their aerenchyma in anaerobic environments. AMF as an endomycorrhizal symbiotic fungus, and part of its hyphae penetrate plant root cells to acquire oxygen (Xu et al. 2016). Therefore, anaerobic or dysoxic conditions would be expected to have little adverse effect on AMF activity and the production of GRSP, and (3) because GRSP can be translocated in water, regular river irrigation in paddy wetlands and reed wetlands may contribute to the deposition of allochthonous GRSP (Harner et al. 2004; Brix et al. 2014; Singh et al. 2017). In contrast, the relatively low GRSP concentrations in the seablite wetlands (Fig. 3a) may be explained by one or more of the following lines of reasoning: (1) vegetation in the seablite wetlands was sparse, and GRSP yields are significantly and positively correlated with primary productivity (Treseder and Turner 2007), (2) the high salinity in the surface soil of the seablite wetlands would not favor survival of AMF (Guo and Gong 2014), and (3) the area is often affected by tidal flushing, and some GRSP may have been leached from the sediments and exported to the ocean (Adame et al. 2010; Wang et al. 2018*a*). Finally, the low GRSP concentrations in the corn fields may have been related to the farming method. The annual replanting and tilling of the soil lead to exposure of the soil to oxygen, which is not conducive to the preservation of GRSP (Spohn and Giani 2010). In addition, the use of chemical fertilizers and pesticides in corn fields may also be detrimental to the AMF production and accumulation of GRSP (Wilson et al. 2009)

There was a significant positive correlation between GRSP concentrations and water content, and a significant negative correlation with BD (Table 2, Supporting Information Figs. S1b, S2d). These correlations were consistent with results of a study in mangrove forests (Wang et al. 2018*b*). To some extent, the correlations could reflect the improvement of soil structure by GRSP. Previous studies have found inconsistent correlations between GRSP concentrations and sediment grain size in different ecosystems (Zhu et al. 2010; Singh et al. 2016; Wang et al. 2018*b*). Zhu et al. (2010) found that the concentrations of GRSP in the soils of five different land use types on Hainan Island were significantly and positively correlated with the percent sand in the soil, and significantly and negatively correlated with the percent silt and clay. They believed that soil with a high sand content was highly permeable to water and air. They reasoned that this permeability would enhance the growth and vitality of roots, the activity of AMF, and could therefore explain the positive correlation between GRSP concentrations and sand content. However, in our study, we found that there was a significant negative correlation between GRSP concentrations and sand content. Instead, there was a significant positive correlation between GRSP concentrations and silt and clay contents (Table 2, Supporting Information Fig. S2a–c). These correlations are consistent with the results reported by Wang et al. (2018*b*). An explanation for the correlations in this study may be that high contents of silt and clay in the sediment contribute to the preservation of GRSP and delay its degradation. In addition, as we have noted above, the vegetation in this study consisted mainly of plants that have aerenchyma that can make oxygen available to AMF. The poor soil permeability caused by the high silt and clay contents might therefore not adversely affect the activity of AMF. The concentrations of GRSP in this area were therefore directly proportional to the clay and silt contents. This relationship in turn led to a positive correlation between the CIA and clay or silt contents at $p < 0.05$ (Table 2).

The GRSP concentrations were positively correlated with SOC, TN, TP, Fe, and other nutrient concentrations in all sediments (Table 2, Supporting Information Figs. S1a,c,d, S3d). A similar correlation between GRSP and SOC and TN has been well documented in several studies (Lovelock et al. 2004; Wang et al. 2018*b*). Many studies, however, have shown that soil P concentrations are negatively correlated with the level of AMF colonization (Anderson et al. 1994; Lin et al. 2012), and only when plant growth is restricted by P, addition of P will increase AMF colonization (Koide and Li 1990). Our study revealed a positive correlation between GRSP and TP concentrations, which presumably reflected the low content of phosphorus in the soil. However, the study sediment contained only 1.20% apatite and 0.64% monazite (He et al. 2016); it did not have contain abundant phosphorus. We therefore hypothesize that the vegetation in this study area was restricted by bioavailable P.

Among the many metals, Fe has a special role in the formation of GRSP. Although the molecular structure of GRSP has not been accurately defined, early studies have reported that GRSP tightly binds Fe, which accounts for 0.04–8.80% of the mass of GRSP. Iron is thus thought to be the most abundant metal in GRSP

(Wright and Upadhyaya 1998) and to account for the reddish-brown color of an alkaline solution of GRSP (Wang et al. 2015). The role of Fe in organic matter suggests that it may contribute to the thermal stability and antimicrobial properties of GRSP (Nichols et al. 2005). In addition, Kemper and Koch (1966) have found that soil aggregation is a function of organic matter content and the abundance of clay particles and free iron oxides. Iron hydroxides may create a link between organic matter and clay minerals to form organic-mineral complexes that can protect organic matter from degradation. The significant positive correlation between GRSP and Fe in the sediment samples (Table 2, Supporting Information Fig. S3d) may therefore reflect their intrinsic linkage.

The concentrations of Na and Cl in the sediments of this study were significantly and negatively correlated with GRSP concentrations (Table 2, Supporting Information Fig. S3a,b). This result is consistent with the study in the Songnen Plain and with other studies (Zhang et al. 2017). Guo and Gong (2014), for example, have found that the spore colonization rate and diversity of AMF decrease with an increase of sediment salinity, and the production of GRSP therefore decreases. Because SO_4^{2-} is one of the major anions in seawater, an increase of salinity in the coastal area would be associated with an increase in the concentration of SO_4^{2-}, which could act as an electron acceptor in the absence of oxygen and accelerate the oxidative decomposition of GRSP (Weston et al. 2011). In addition, the Na^+ and Cl^- ions have small ionic radii compared to ammonium and phosphate, respectively, and might be preferentially transported to host plants. The result would be a reduction of AMF colonization due to nutrient limitation of plant growth. Changes of salinity can therefore have a great impact on the production and degradation of GRSP. The implication is that sea level rise may have a negative impact on the accumulation of GRSP, and in turn adversely impact carbon sequestration in coastal wetlands.

The pH of the sediment is a very important abiotic determinant of AMF colonization and GRSP production (Guo and Gong 2014; Wang et al. 2015). Previous studies have shown that neutral and weakly acidic sediments favor the accumulation of GRSP (Wang et al. 2013). In addition, Bago et al. (1996) have found that the extraradical mycelium of AMF can secrete organic acids to reduce the pH of the rhizospheres, thereby increasing the bioavailability of K, Ca, Mg, and Fe for absorption by host plants. However, there was no significant relationship between the pH and GRSP concentrations in this study (Table 2). The pH of the study area, 7.7–10.1, was weakly alkaline. Therefore, secretion of weakly acidic organic acids by the AMF may have had little influence on GRSP production. Still, the pH of sediment is affected by many factors, of which AMF is only one. In this study, the effect of AMF on pH may have been negligible.

The aforementioned analyses suggest that effective management can improve the acquisition of mineral nutrients and in turn enhance soil carbon sequestration in wetland ecosystems. The main management strategies proposed here include (1) reducing the conversion of wetlands into agricultural lands, or maintaining agricultural lands as always wet (such as rice paddy) can effectively improve AMF colonization and increase GRSP accumulation, (2) maintaining the surface elevation of wetlands to reduce the invasion of seawater, that is, to reduce the invasion of Na and Cl ions into ecosystems, is instrumental in GRSP preservation and accumulation, (3) increasing vegetation coverage in the watershed and reducing the loss of soluble organic matter due to the long-term transport of SOC, and decreasing the amount of carbon rereleased into the atmosphere, thereby to reduce the GRSP/SOC ratio, (4) restoring vegetated wetlands to increase weathering intensity, thus obtaining nutrients from minerals and promoting plant growth, so as to achieve the goal of enhancing carbon sequestration, and (5) filling fine grain size sediments in soil surface when wetlands covered by plants that have aerenchyma or adding P fertilizer in P-constrained ecosystems are also applicable to improve AMF colonization, GRSP concentration, and thus to enhance carbon sequestration in coastal wetland ecosystems.

References

Adame, M. F., D. Neil, S. F. Wright, and C. E. Lovelock. 2010. Sedimentation within and among mangrove forests along a gradient of geomorphological settings. Estuar. Coast. Shelf Sci. **86**: 21–30. doi:10.1016/j.ecss.2009.10.013

Anderson, R. C., H. Bad, and W. Gwt. 1994. Mycorrhizal dependence of *Andropogon gerardii* and *Schizachyrium scoparium* in two prairie soils. Am. Midl. Nat. **132**: 366–376. doi:10.2307/2426592

April, R., and R. Newton. 1992. Mineralogy and mineral weathering, p. 378–425. *In* D. W. Johnson and S. E. Lindberg [eds.], Atmospheric deposition and forest nutrient cycling. Ecological studies (analysis and synthesis), v. **91**. Springer.

Arocena, J. M., B. Velde, and S. J. Robertson. 2012. Weathering of biotite in the presence of arbuscular mycorrhizae in selected agricultural crops. Appl. Clay Sci. **64**: 12–17. doi: 10.1016/j.clay.2011.06.013

Bago, B., H. Vierheilig, Y. PichÉ, and C. Azcón-Aguilar. 1996. Nitrate depletion and pH changes induced by the extraradical mycelium of the arbuscular mycorrhizal fungus *Glomus intraradices* grown in monoxenic culture. New Phytol. **133**: 273–280. doi:10.1111/j.1469-8137.1996.tb01894.x

Bai, C., X. He, H. Tang, B. Shan, and L. Zhao. 2009. Spatial distribution of arbuscular mycorrhizal fungi, glomalin and soil enzymes under the canopy of *Astragalus adsurgens* Pall. in the Mu Us sandland, China. Soil Biol. Biochem. **41**: 941–947. doi:10.1016/j.soilbio.2009.02.010

Berner, R. A. 1997. The rise of plants and their effect on weathering and atmospheric CO_2. Science **276**: 506–511.

Bird, S. B., J. E. Herrick, M. M. Wander, and S. F. Wright. 2002. Spatial heterogeneity of aggregate stability and soil carbon in semi-arid rangeland. Environ. Pollut. **116**: 445–455. doi:10.1016/S0269-7491(01)00222-6

Brix, H., and others. 2014. Large-scale management of common reed, *Phragmites australis*, for paper production: A case study from the Liaohe Delta, China. Ecol. Eng. **73**: 760–769. doi:10.1016/j.ecoleng.2014.09.099

Caravaca, F., M. d. M. Alguacil, P. Torres, and A. Roldán. 2005. Microbial activities and arbuscular mycorrhizal fungi colonization in the rhizosphere of the salt marsh plant *Inula crithmoides* L. along a spatial salinity gradient. Wetlands **25**: 350–355. doi:10.1672/11

Driver, J. D., W. E. Holben, and M. C. Rillig. 2005. Characterization of glomalin as a hyphal wall component of arbuscular mycorrhizal fungi. Soil Biol. Biochem. **37**: 101–106. doi:10.1016/j.soilbio.2004.06.011

Gillespie, A. W., and others. 2011. Glomalin-related soil protein contains non-mycorrhizal-related heat-stable proteins, lipids and humic materials. Soil Biol. Biochem. **43**: 766–777. doi:10.1016/j.soilbio.2010.12.010

Guo, X., and J. Gong. 2014. Differential effects of abiotic factors and host plant traits on diversity and community composition of root-colonizing arbuscular mycorrhizal fungi in a salt-stressed ecosystem. Mycorrhiza **24**: 79–94.

Harner, M. J., P. W. Ramsey, and M. C. Rillig. 2004. Protein accumulation and distribution in floodplain soils and river foam. Ecol. Lett. **7**: 829–836. doi:10.1111/j.1461-0248.2004.00638.x

He, L., and others. 2016. Distribution of detrital minerals in the core ZK2 at the Liaohe Delta area since Late Pleistocene: Implication for provenance. Mar. Geol. Quat. Geol. **36**: 23–32.

He, X., Y. Li, and L. Zhao. 2010. Dynamics of arbuscular mycorrhizal fungi and glomalin in the rhizosphere of *Artemisia ordosica* Krasch. in Mu Us sandland, China. Soil Biol. Biochem. **42**: 1313–1319. doi:10.1016/j.soilbio.2010.03.022

Johansen, A., I. Jakobsen, and E. S. Jensen. 1993. Hyphal transport by a vesicular-arbuscular mycorrhizal fungus of N applied to the soil as ammonium or nitrate. Biol. Fertil. Soils **16**: 66–70. doi:10.1007/BF00336518

Johnson, D. W., and others. 1982. Nutrient cycling in forests of the Pacific Northwest p. 186–232. In R. L. Edmonds [eds.], Analysis of Coniferous forest ecosystems in the western United States. US/IBP Synthesis series 14. Hutchinson Post Publishing Company.

Jongmans, A. G., and others. 1997. Rock-eating fungi. Nature **389**: 682. doi:10.1038/39493

Kemper, W. D., and E. J. Koch. 1966. Aggregate stability of soils from western United States and Canada. Measurement procedure, correlation with soil constituents, v. **1**. U.S. Government Printing Office, p. 1–51.

Kleber, M., P. Sollins, and R. Sutton. 2007. A conceptual model of organo-mineral interactions in soils: Self-assembly of organic molecular fragments into zonal structures on mineral surfaces. Biogeochemistry **85**: 9–24.

Koele, N., I. A. Dickie, J. D. Blum, J. D. Gleason, and L. de Graaf. 2014. Ecological significance of mineral weathering in ectomycorrhizal and arbuscular mycorrhizal ecosystems from a field-based comparison. Soil Biol. Biochem. **69**: 63–70. doi:10.1016/j.soilbio.2013.10.041

Koide, R. T., and M. G. Li. 1990. On host regulation of the vesicular-arbuscular mycorrhizal symbiosis. New Phytol. **114**: 59–74. doi:10.1111/j.1469-8137.1990.tb00373.x

Lin, X., and others. 2012. Long-term balanced fertilization decreases arbuscular mycorrhizal fungal diversity in an arable soil in North China revealed by 454 pyrosequencing. Environ. Sci. Technol. **46**: 5764–5771. doi:10.1021/es3001695

Liu, J., and others. 2017. Metal pollution across the upper delta plain wetlands and its adjacent shallow sea wetland, northeast of China: Implications for the filtration functions of wetlands. Environ. Sci. Pollut. Res. **25**: 1–16.

López-Merino, L., O. Serrano, M. F. Adame, M. Á. Mateo, and A. Martínez Cortizas. 2015. Glomalin accumulated in seagrass sediments reveals past alterations in soil quality due to land-use change. Global Planet. Change **133**: 87–95. doi:10.1016/j.gloplacha.2015.08.004

Lovelock, C. E., S. F. Wright, D. A. Clark, and R. W. Ruess. 2004. Soil stocks of glomalin produced by arbuscular mycorrhizal fungi across a tropical rain forest landscape. J. Ecol. **92**: 278–287. doi:10.1111/j.0022-0477.2004.00855.x

McLennan, S. M. 1993. Weathering and global denudation. J. Geol. **101**: 295–303. doi:10.1086/648222

Mitsch, W., and J. Gosselink. 2007. Wetlands, 4nd ed. Wilely.

Mo, B., and B. Lian. 2010. Study on feldspar weathering and analysis of relevant impact factors. Earth Sci. Front. **17**: 281–289.

Nesbitt, H. W., G. Markovics, and R. C. Price. 1980. Chemical processes affecting alkalis and alkaline earths during continental weathering. Geochim. Cosmochim. Acta **44**: 1659–1666. doi:10.1016/0016-7037(80)90218-5

Nesbitt, H. W., and G. M. Young. 1982. Early Proterozoic climates and plate motions inferred from major element chemistry of lutites. Nature **299**: 715. doi:10.1038/299715a0

Nesbitt, H. W., G. M. Young, S. M. McLennan, and R. R. Keays. 1996. Effects of chemical weathering and sorting on the petrogenesis of siliciclastic sediments, with implications for provenance studies. J. Geol. **104**: 525–542. doi:10.1086/629850

Nichols, A. K., and S. F. Wright. 2005. Comparison of glomalin and humic acid in eight native U.S. soils. Soil Sci. **170**: 985–997. doi:10.1097/01.ss.0000198618.06975.3c

Olsen, S., and L. Sommers. 1982. Phosphorus methods of soil analysis. Part 2: Chemical and microbiological properties, 2nd ed. American Society of Agronomy.

Preger, A. C., M. C. Rillig, A. R. Johns, P. C. Du, I. Lobe, and W. Amelung. 2007. Losses of glomalin-related soil protein under prolonged arable cropping: A chronosequence study in sandy soils of the South African Highveld. Soil Biol. Biochem. **39**: 445–453. doi:10.1016/j.soilbio.2006.08.014

Rillig, M. C. 2004. Arbuscular mycorrhizae, glomalin, and soil aggregation. Can. J. Soil Sci. **84**: 355–363. doi:10.4141/S04-003

Rillig, M. C., F. T. Maestre, and L. J. Lamit. 2003*a*. Microsite differences in fungal hyphal length, glomalin, and soil aggregate stability in semiarid Mediterranean steppes. Soil Biol. Biochem. **35**: 1257–1260.

Rillig, M. C., P. W. Ramsey, S. Morris, and E. A. Paul. 2003*b*. Glomalin, an arbuscular-mycorrhizal fungal soil protein, responds to land-use change. Plant Soil **253**: 293–299.

Sanz-Montero, M. E., and J. P. Rodríguez-Aranda. 2012. Endomycorrhizae in Miocene paleosols: Implications in biotite weathering and accumulation of dolomite in plant roots (SW Madrid Basin, Spain). Palaeogeogr. Palaeoclimatol. Palaeoecol. **333–334**: 121–130. doi:10.1016/j.palaeo.2012.03.013

Singh, A. K., A. Rai, and N. Singh. 2016. Effect of long term land use systems on fractions of glomalin and soil organic carbon in the Indo-Gangetic plain. Geoderma **277**: 41–50. doi:10.1016/j.geoderma.2016.05.004

Singh, A. K., A. Rai, V. Pandey, and N. Singh. 2017. Contribution of glomalin to dissolve organic carbon under different land uses and seasonality in dry tropics. J. Environ. Manage. **192**: 142–149. doi:10.1016/j.jenvman.2017.01.041

Singh, P. K., M. Singh, and B. N. Tripathi. 2013. Glomalin: An arbuscular mycorrhizal fungal soil protein. Protoplasma **250**: 663–669. doi:10.1007/s00709-012-0453-z

Spohn, M., and L. Giani. 2010. Water-stable aggregates, glomalin-related soil protein, and carbohydrates in a chronosequence of sandy hydromorphic soils. Soil Biol. Biochem. **42**: 1505–1511. doi:10.1016/j.soilbio.2010.05.015

Treseder, K. K., and K. M. Turner. 2007. Glomalin in ecosystems. Soil Sci. Soc. Am. J. **71**: 1257–1266. doi:10.2136/sssaj2006.0377

Wang, C. Y., and others. 2013. Glomalin-related soil protein distribution and its environmental affecting factors in the Northeast Inner Mongolia. Arid Zone Res. **30**: 22–28.

Wang, Q., and others. 2014. Spatial variations in concentration, compositions of glomalin related soil protein in poplar plantations in northeastern China, and possible relations with soil physicochemical properties. ScientificWorldJournal **2014**: 160403. doi:10.1155/2014/160403

Wang, Q., W. Wang, X. He, W. Zhang, K. Song, and S. Han. 2015. Role and variation of the amount and composition of glomalin in soil properties in farmland and adjacent plantations with reference to a primary forest in North-Eastern China. PLoS One **10**: e0139623. doi:10.1371/journal.pone.0139623

Wang, Q., and others. 2018*a*. Glomalin-related soil protein deposition and carbon sequestration in the Old Yellow River delta. Sci. Total Environ. **625**: 619–626.

Wang, Q., and others. 2018*b*. Spatial distribution of glomalin-related soil protein and its relationship with sediment carbon sequestration across a mangrove forest. Sci. Total Environ. **613–614**: 548–556.

Weston, N. B., S. C. Neubauer, and D. J. Velinsky. 2011. Accelerated microbial organic matter mineralization following salt-water intrusion into tidal freshwater marsh soils. Biogeochemistry **102**: 135–151. doi:10.1007/s10533-010-9427-4

Wilson, G. W. T., C. W. Rice, M. C. Rillig, A. Springer, and D. C. Hartnett. 2009. Soil aggregation and carbon sequestration are tightly correlated with the abundance of arbuscular mycorrhizal fungi: Results from long-term field experiments. Ecol. Lett. **12**: 452–461. doi:10.1111/j.1461-0248.2009.01303.x

Wright, S. F., M. Franke-Snyder, J. B. Morton, and A. Upadhyaya. 1996. Time-course study and partial characterization of a protein on hyphae of arbuscular mycorrhizal fungi during active colonization of roots. Plant Soil **181**: 193–203. doi:10.1007/BF00012053

Wright, S. F., and A. Upadhyaya. 1998. A survey of soils for aggregate stability and glomalin, a glycoprotein produced by hyphae of arbuscular mycorrhizal fungi. Plant Soil **198**: 97–107. doi:10.1023/A:1004347701584

Wright, S. F., and R. L. Anderson. 2000. Aggregate stability and glomalin in alternative crop rotations for the central Great Plains. Biol. Fertil. Soils **31**: 249–253. doi:10.1007/s003740050653

Wright, S. F., K. A. Nichols, and W. F. Schmidt. 2006. Comparison of efficacy of three extractants to solubilize glomalin on hyphae and in soil. Chemosphere **64**: 1219–1224. doi:10.1016/j.chemosphere.2005.11.041

Xie, H., and others. 2015. Long-term manure amendments reduced soil aggregate stability via redistribution of the glomalin-related soil protein in macroaggregates. Sci. Rep. **5**: 14687.

Xu, Z., Y. Ban, Y. Jiang, X. Zhang, and X. Liu. 2016. Arbuscular mycorrhizal fungi in wetland habitats and their application in constructed wetland: A review. Pedosphere **26**: 592–617. doi:10.1016/S1002-0160(15)60067-4

Yang, S., and others. 2019. Regional-scale distributions of pollen and spore assemblages in alluvium around the Bohai Sea: An essential step toward understanding marine palynological sources in China. Mar. Geol. **415**: 105968. doi:10.1016/j.margeo.2019.105968

Ye, S., and others. 2015. Carbon sequestration and soil accretion in coastal wetland communities of the Yellow River

Delta and Liaohe Delta, China. Estuaries Coast. **38**: 1885–1897. doi:10.1007/s12237-014-9927-x

Ye, S., and others. 2016*a*. Inter-annual variability of area-scaled gaseous carbon emissions from wetland soils in the Liaohe Delta, China. PLoS One **11**: e0160612.

Ye, S., and others. 2016*b*. Carbon sequestration and soil accretion in coastal wetland communities of the Yellow River Delta and Liaohe Delta, China. Estuaries Coast. **39**: 294–294.

Zhang, S., Q. Li, X. Zhang, K. Wei, L. Chen, and W. Liang. 2012. Effects of conservation tillage on soil aggregation and aggregate binding agents in black soil of Northeast China. Soil Tillage Res. **124**: 196–202. doi:10.1016/j.still.2012.06.007

Zhang, Z., Q. Wang, H. Wang, S. Nie, and Z. Liang. 2017. Effects of soil salinity on the content, composition, and ion binding capacity of glomalin-related soil protein (GRSP). Sci. Total Environ. **581**: 657–665.

Zhu, F., Q. H. Zhao, W. G. Deng, and M. Z. Chen. 2010. Relationships among glomalin related soil protein, SOC and soil texture under different land use tyoes. J. Anhui Agric. Sci. **38**: 12499–12502.

Acknowledgment

We thank Guangming Zhao, Xigui Ding, Jin Liu, Lei He, and Shixiong Yang and other staff for the hard working in the field and in the laboratory. In addition, this manuscript benefitted greatly from the constructive comments of two anonymous reviewers. This study was jointly funded by the National Key R&D Program of China (2016YFE0109600), Ministry of Land and Resources program: "Special foundation for scientific research on public causes" (Grant 201111023), National Natural Science Foundation of China (Grant 41240022 and 40872167), and China Geological Survey (Grant DD20189503, 1212010611402, GZH201200503, and DD20160144).

Conflict of Interest

None declared.

Submitted 09 December 2018
Revised 09 July 2019
Accepted 27 September 2019

Associate editor: James Leichter